Canadian Journal of Fisheries and Aquatic Sciences
Journal canadien des sciences halieutiques et aquatiques

Can a bottom-moored echosounder array provide a survey-comparable index of abundance?

Journal:	*Canadian Journal of Fisheries and Aquatic Sciences*
Manuscript ID	cjfas-2017-0013.R2
Manuscript Type:	Article
Date Submitted by the Author:	29-May-2017
Complete List of Authors:	De Robertis, Alex; National Marine Fisheries Service - NOAA, Alaska Fisheries Science Center Levine, Robert; University of Washington , School of Oceanography Wilson, Christopher; National Marine Fisheries Service, AFSC
Is the invited manuscript for consideration in a Special Issue? :	N/A
Keyword:	ACOUSTICS < General, Moorings, Gadus chalcogrammus, Shelikof Strait, INSTRUMENTATION < General

Can a bottom-moored echosounder array provide a survey-comparable index of abundance?

Alex De Robertis[1*], Robert Levine[1†], Christopher D. Wilson [1‡]

[1] National Marine Fisheries Service, 7600 Sand Point Way NE, Seattle WA 98115, USA

* Corresponding author: Alex.DeRobertis@noaa.gov, Tel: (206) 526-4789, Fax: (206) 526-6723

† Current address, University of Washington, School of Oceanography, 1503 NE Boat St., Seattle, WA 98105, USA. leviner@uw.edu

‡Chris.Wilson@noaa.gov

Abstract

A small number of stationary echosounders have the potential to produce abundance indices where fish repeatedly occupy localized areas (e.g., spawning grounds). To investigate this possibility, we deployed three trawl-resistant moorings with a newly-designed autonomous echosounder for ~85 days during the walleye pollock spawning season in Shelikof Strait, Alaska. Backscatter observed from the moorings was highly correlated with ship-based acoustic surveys, suggesting that the mooring observations reflect abundance over much larger areas than the observation volume of the acoustic beam. A retrospective analysis of a 19-year time series of pre-spawning pollock surveys was used to select mooring locations and determine that 3-5 moorings can produce an index of pollock backscatter comparable to that produced by a ship-based survey covering ~18,000 km^2 (mean prediction error of <11% for 5 moorings). The three moorings deployed in Shelikof Strait yielded a backscatter estimate that was within ~15-20% of that observed during the survey. Thus, it appears feasible to design a relatively sparse mooring array to provide abundance information and other aspects of fish behavior in this environment.

Introduction

Autonomous or cabled echosounders that can be deployed on the sea floor for extended periods are increasingly available. These instruments are effective tools to study diel and seasonal trends in the abundance and behavior of fish and zooplankton (Trevorrow, 2005; Kaartvedt et al., 2009; Ross et al., 2013). Bottom-mounted acoustic measurements can potentially be used to generate low-cost abundance indices of fish. Many fishes aggregate in predictable and restricted areas, particularly for spawning (Lawson and Rose, 2000; Doonan et al., 2003) and overwintering (Løland et al., 2007; Benoit et al., 2008), and this approach may have widespread application. Stationary echosounders can also be used to quantify the formation, duration, and dispersal of fish aggregations (Kaltenberg et al., 2010). This is important information for ship-based surveys, as the timing of surveys relative to the timing of aggregation is often a major source of uncertainty in surveys of spawning fish (Nelson and Nunnallee, 1984; O'Driscoll, 2004). However, it remains uncertain how many echosounder moorings would be needed to provide useful indices of abundance in a given survey area, and where these echosounders should be located.

The primary outstanding question regarding the utility of echosounder moorings for abundance estimation is the degree to which temporally averaged measurements from stationary instruments represent the density of fishes over a wide area. Although echosounder moorings image a relatively small area compared to ship-based surveys, time-averaged observations from a stationary sensor can represent the abundance over a broad area, due to spatial correlation in animal distributions and the movements of organisms relative to the sensor (e.g., Brierley et al., 2006). The degree to which observations from an upward-looking echosounder can be extrapolated over a broad spatial area is difficult to quantify and case-specific. Knowledge of the degree to which the mooring data represent abundance in a broader area than the acoustic beam is critical for the design of a moored echosounder network (i.e., determine the appropriate number and placement of moorings). It is thus unclear if a relatively sparse array of a few echosounder moorings can be used to provide a useful index of abundance over a large spatial area.

Here, we evaluate the utility of bottom-moored echosounders to monitor the abundance of walleye pollock (*Gadus chalcogrammus*) in Shelikof Strait, an important spawning location in the Gulf of Alaska. An annual acoustic-trawl survey covering ~1,500 km of transects (Nelson and Nunnallee, 1984; Wilson, 1994; McCarthy et al., 2015) is conducted in a ~18,000 km^2 area to manage the fishery (Dorn et al., 2015). As a first step, we evaluate the possibility of using a small number of moorings to generate an index of acoustic backscatter comparable to that produced by the ship-based survey. The key questions to be addressed are how many moorings are needed to generate an abundance index in a wider area, and where the moorings should be located. Thus, the principal goals of this work are to characterize the spatial sampling dimension of a moored echosounder in Shelikof Strait, and estimate uncertainty in the abundance index as a function of number of moorings. We combine a series of observations from echosounder moorings deployed on the seafloor, ship-based surveys conducted while the moorings were deployed, and a retrospective analysis of the survey time series to address these questions.

Methods

1.1 Approach

We deployed three echosounder moorings on the seafloor in Shelikof Strait, Alaska (section 1.2). Pollock dominate the backscatter in this area during the spring spawning period (Nelson and Nunnallee, 1984; McCarthy et al., 2015). For example, 98.8 ± 1.4% (mean ± SD) of the observed backscatter during annual acoustic-trawl surveys was attributed to pollock based on examination of echograms and trawl sampling (estimates are for 2003 to 2015 when this was quantified). We conducted repeated surveys with vessel-mounted echosounders at two spatial scales, a 50 nmi^2 (nautical mile) area centered over the mooring sites, and coarse-scale surveys of the entire Strait (section 1.3). We compare the observations from the echosounder moorings to those from the ship surveys to examine whether the observations from the moorings were correlated with the ship-based surveys at these larger spatial scales (section 1.4). We also conduct a retrospective analysis of a time series (1995-2015) of acoustic surveys in the area in which we use survey data as a proxy for mooring data to determine the number and locations of moorings needed to generate an acoustic abundance index in Shelikof Strait (section 1.5). Finally, we use the mooring observations combined with the method developed in the retrospective analysis to predict the backscatter observed during the 2015 survey (section 1.6).

1.2 Echosounder moorings

Three echosounder moorings were placed on the seafloor in Shelikof Strait at depths of 260-294 m during the 2015 spawning season to observe the arrival and dispersal of pollock spawning aggregations (Fig. 1, details in Table S1). One mooring was deployed in each of the northern, the central, and the southern sectors of Shelikof Strait (hereafter referred to as the north, central and south moorings) on 12-19 February and recovered on 7-8 May (Fig. 1, Table S1). The mooring locations were selected based on logistics, previous survey results, input from participants in the fishery, and a preliminary version of the analysis described in section 1.5.

The moorings were deployed in areas with an active fishery, and were thus constructed to be trawl-resistant. We modified low-profile trawl-resistant bottom mount housings (178 x 127 x 56 cm) manufactured by Mooring Systems for use with an EdgeTech PORT-LF acoustic release and a sacrificial steel weight (229 kg , 122 x 37 x 2.5 cm). Eight 36 cm diameter trawl floats were used to bring the mooring to the sea surface during recovery. The moorings were instrumented with prototype battery-powered split-beam wideband autonomous transceivers (WBATs) developed by Simrad AS equipped with newly-designed 70 kHz 18 degree depth-rated transducers (model ES70-18CD). The transducers were mounted in a two-axis gimbal equipped with a 0.7 kg counterweight below the transducer which served to keep the transducer oriented towards the sea surface.

To account for pressure effects on calibration, the on-axis sensitivity of each WBAT was calibrated at the approximate deployment depth by lowering it on a frame with the transducer mounted in a down-facing 2-axis gimbal. A 16 m line with a 38.1 mm tungsten-carbide calibration sphere at a distance of 12 m and a 5 kg lead weight at the end was suspended from the transducer. The gimbal and weight served to keep the transducer pointing downward and the sphere near the center of the beam. The instruments were lowered to 270 m and 700-1000 pings were collected. We estimated the echosounder gain using the on-axis method (Demer et al., 2015), and used this for post-processing.

During the deployment, the WBATs were programmed to transmit an ensemble of 200 pings at the beginning of each hour at a ping interval of 2 s from the time of deployment to 1 May 2015. A 1 ms 70 kHz narrowband pulse with a transmit power of 400 W was used. Data were recorded to 325 m. After May 1, an ensemble was transmitted every 6 hours. The nautical area backscattering coefficient (s_A, m^2 nmi^{-2}, MacLennan et al., 2002) from the WBATs was echo-integrated using a -70 dB re 1 m^{-1} integration threshold from 2 m from the transducer to 10 m below the surface echo.

1.3 Ship surveys and trawl sampling

Ship-based acoustic surveys were conducted at two scales to describe the temporal changes in pollock abundance during the mooring deployment. We conducted 'coarse-scale' surveys of the Shelikof Strait survey area (Fig. 1, gray lines), and 'small-scale' surveys in the vicinity of each of the mooring sites (Fig. 1 inset). The acoustic surveys were conducted with calibrated 38 kHz Simrad EK60 echosounders equipped with model ES38B split-beam transducers mounted on a centerboard (NOAA Ship *Oscar Dyson*) or the vessel's hull (F/V *Mar Del Norte*). Backscatter was measured from 16 m to 0.5 m above the bottom using a -70 dB re 1 m^{-1} integration threshold (McCarthy et al., 2015).

We determined that the acoustic backscatter observed on a coarse-scale survey covering five transect lines was well-correlated with that of the survey as a whole over the last two decades (Fig. S1). This allowed us to conduct four replicate coarse-scale surveys as the vessels transited through Shelikof Strait in 2015 which could be compared with the mooring observations. Surveys were conducted with the NOAA Ship *Oscar Dyson* on 25-26 February, on 17-23 March, and 27-30 March, and with the F/V *Mar Del Norte* on 6-10 March.

The small-scale surveys consisted of three 10 nmi transects in a 50 nmi^2 (i.e. 5 by 10 nmi) area centered on the mooring position and 1-2 diagonal transects across the survey area (Fig. 1). The surveys were conducted when the vessel passed by the mooring locations during each of the four coarse-scale surveys. The north mooring was surveyed four additional times for a total of eight surveys (2 surveys on 2 March, and two on 30 March). A pelagic trawl (*Oscar Dyson*: Aleutian Wing Trawl ~25 by 35 m mouth opening, *Mar Del Norte*: Mirek trawl ~27 by 45 m mouth opening) equipped with a 1.2 cm codend liner was fished at the depth and location of the greatest backscatter observed each date a mooring was deployed, recovered, or visited except (n = 16, trawl durations 7-61 min). The catch was sorted and measured as described in McCarthy et al. (2015). The proportion of the backscatter attributable to pollock at each trawl site was estimated by combining the trawl catch composition and estimates of target strength as described in De Robertis et al. (2017).

1.4 Comparison of data from ships and moorings

All available vessel observations within the 50 nmi^2 small-scale surveys were compared with the average backscatter observed by the WBAT during the time it took the ship to complete the small-scale survey (2-5 hours). In May, when data were collected every 6 hours, the closest 200 ping ensemble was used. Backscatter at 38 kHz was used to represent the ship as 70 kHz data are not available from the *Mar Del Norte* and most of the 19-year time series used to determine mooring locations (see section 1.5). Pollock abundance in Shelikof Strait is highly depth-dependent (e.g. McCarthy et al., 2015) and the mooring measurements are thus specific to the depth of the mooring (i.e. a mooring at the deepest point of the strait conveys little information about pollock abundance at shallower depths). We thus restricted the ship survey to areas where the observed bottom depth was within 10% of the mooring depth. This criterion did not exclude data from the south and central mooring sites, but excluded 10.2% of the small-scale survey around the north mooring. We applied the method of Kieser et al. (1987) to estimate the mean and 95% confidence intervals for the ratio of backscatter (R) observed by the moorings at 70 kHz and the survey vessels at 38 kHz (i.e. $s_{A,vessel}$ / $s_{A,mooring}$). This method treats each mooring survey (n = 16) as a sample unit.

1.5 Retrospective analysis of surveys to select mooring locations

We used 19 surveys of pre-spawning pollock in Shelikof Strait conducted from 1995-2015 (no surveys in 1999 and 2011) to develop an objective method to establish the number and locations of echosounder moorings required to produce an abundance index in the 18,000 km^2 Shelikof Strait survey area, and combine information from multiple moorings. The goal was to use existing survey data as a proxy for ‘virtual moorings’ to determine whether observations in a limited number of locations could be used to develop an index of pollock backscatter.

Acoustic backscatter for the surveys is available every 0.5 nmi (McCarthy et al., 2015). The survey area was divided into 7 by 7 nmi grid cells (the smallest scale at which cells were consistently visited in all the surveys), and ship observations in these cells were used to represent the observations from a virtual mooring. We considered this to be justified as the mooring observations were highly correlated with ship surveys in a 50 nmi^2 area during the 2015 mooring deployments (see section 2.3). In Shelikof Strait, pollock abundance tends to increase with depth. We thus placed the virtual moorings at the deepest point visited in each grid cell. All ship backscatter measurements in the cell within 10% of the bottom depth of the mooring were averaged and used to represent the observations from the virtual mooring.

Survey coverage varied slightly among years. Some transects at the northern and southern ends of the survey area were not completed in all years, and in recent years the transects have a random starting location (i.e. transects shift position by up to ± 3.5 nmi). A total of 99 cells were visited in all years of the survey, which encompasses 82.8 ± 4.0% (mean ± SD) of the trackline sampled in each year. These cells account for 94.4 ± 4.4% of the total backscatter observed in a given survey.

We used a stratification scheme to ensure that the ‘virtual moorings’ were broadly dispersed over Shelikof Strait. The survey area was divided into *n* spatially contiguous strata, where *n* varied from 1 to 5. A single virtual mooring was allocated to each stratum to represent the use of 1-5 echosounder moorings in Shelikof Strait. The size of each stratum was determined by first computing the proportion of the survey backscatter in each cell in a given year, and averaging this proportion across years. Cells were allocated to a stratum until 1/n of the normalized backscatter was observed in that stratum. For example, in the 3-stratum case, 3 areas were delineated corresponding to northern, middle and southern portions of Shelikof Strait in which 1/3 of the backscatter was historically observed (see Fig. S2 for details).

We restricted potential mooring locations to areas of consistent abundance as these areas are more likely to represent the population as a whole. We computed an index to identify cells where pollock backscatter was consistently high. The backscatter observed in a given cell was compared to the median backscatter observed in the stratum containing the cell:

$$BI_{c,y} = \frac{B_{c,y}}{Bmed_{c,y}} \qquad (1)$$

where $B_{c,y}$ is the mean backscatter in cell c in year y and $Bmed_{c,y}$ is the median backscatter in the stratum containing cell c in year y. Only cells where $BI_{c,y} > 1$ for at least 10 years of the 19-year time series were considered as potential mooring locations. This criterion eliminated many of the shallow and low-abundance locations as potential mooring locations (Fig. S2). A list of potential mooring locations was generated by selecting all possible combinations of mooring locations in which one mooring is drawn from each stratum for locations where $BI_{c,y} > 1$ for at least 10 years. Preliminary analyses indicated that selection of mooring locations (explained below) was not sensitive to exclusion of these low-abundance locations. For example, for 3 virtual moorings, the same mooring sites were identified when the *BI* criterion was not applied, even though 5 times more combinations of mooring sites were tested.

A linear model was used to predict the survey-wide backscatter from observations near the mooring sites:

$$s_{A,pred,y} = a_1 \cdot s_{A,m1,y} + a_2 \cdot s_{A,m2,y} + a_3 \cdot s_{A,m3,y} + a_4 \cdot s_{A,m4,y} + a_5 \cdot s_{A,m5,y} + e \quad (2)$$

where y represents the year, $s_{A,pred,y}$ is the survey-wide backscatter estimate derived by considering only the virtual mooring locations in year y in the fitting data set. Each virtual mooring is represented by the cell-averaged shipboard measurements, the a terms are fitted parameters constrained to be positive, and e is a normally distributed error term. When < 5 moorings were considered, the terms representing the additional moorings were omitted.

Optimal mooring locations were identified by finding the combination of virtual moorings producing models with the lowest residual deviance (Nelder and Wedderburn, 1972). To avoid overfitting, the model was evaluated out of sample such that predictions for each survey year were made by excluding the data from that year when determining the mooring locations and a parameters. This resulted in 19 sets of mooring locations and parameters, one for each survey year. Because the model was fit by considering all possible combinations which increased rapidly with the number of moorings considered (i.e. an exhaustive search was employed), the simulations considered 1-5 virtual moorings. The mean absolute percent prediction error for each year was computed as

$$APPE_y = |\left(Survey_{s_{A,pred,y}} / Survey_{s_{A,obs,y}}\right) - 1| \cdot 100 \quad (3)$$

where $Survey_{s_{A,obs,y}}$ corresponds to the ship survey backscatter observed in year y.

1.6 Prediction of the 2015 survey with mooring observations

We generated out-of-sample predictions of 2015 survey backscatter using the 3 moorings deployed in Shelikof Strait. The survey-wide backscatter was predicted with a modified version of eq. 2 adapted to the mooring deployments

$$s_{A,survey,2015} = 0.149(s_{A,m1,d} \cdot R) + 0.249(s_{A,m2,d} \cdot R) + 0.133(s_{A,m3,d} \cdot R) \quad (4)$$

where $s_{A,survey,\ 2015}$ is the backscatter predicted for the 2015 survey, and $s_{A,m1,d}$ is the backscatter observed at mooring 1 on day d, and R is the ship/mooring s_A ratio estimated when comparing the concurrent mooring and ship-based mooring surveys (1.32; see section 2.3). Thus, the prediction depends on the mean daily WBAT backscatter observations and the a_{1-3} coefficients which have been fit with the 1994-2014 'virtual moorings', and R which accounts for the difference in frequency (70 kHz vs. 38 kHz) and geometry (up-looking vs. down-looking) between the mooring and survey.

Results

2.1 Ship surveys and trawl sampling

The four coarse-scale surveys indicated that pollock backscatter in Shelikof Strait was elevated from February to March (Fig. 3A-C), and decreased substantially by early May (Fig. 3D). The surveys suggest that pollock distributions were changing within the Strait: abundance was higher towards the southern part of Shelikof Strait on Feb 25-26 (Fig. 3A), farther north in mid-March (Fig. 3B), and farther to the south in late March (Fig. 3C). During the full acoustic-trawl survey, pollock were most abundant in the central part of the strait on the western side (Fig. 2).

Trawl sampling suggests that the backscatter was dominated by scattering from walleye pollock. Pollock comprised the majority of the catch of the trawls at the mooring sites (74.9% of total catch by weight), and averaged 76.9% of catch weight in individual hauls (range 18.2-99.8%). Squid and eulachon, (*Thaleichthys pacificus*) were commonly captured at the mooring sites, and accounted for 7.4% and 16.9% of total catch by weight, respectively. These species lack gas-filled structures, and thus often exhibit small contributions to total backscatter in the presence of fishes with swimbladders (e.g. De Robertis et al., 2017). When the abundance of animals in the trawl hauls and their sizes and scattering characteristics are considered jointly, on average, 95.5% of the backscatter (83-100% for individual hauls) is attributed to pollock.

2.2 Mooring observations

Aggregation patterns typical of pre-spawning pollock were evident in the mooring records, and there was evidence of rapid changes in local abundance (Fig. 4). The observations at the moorings indicated that pollock distributions were changing during the spawning season. Backscatter at the north mooring was low in February, increased to high levels until mid-March and then declined to low levels by the end of March (Figs. 4, 5A). Backscatter at the north mooring was high for ~10 days in early March and then declined abruptly on March 17, ~2 days prior to when the survey visited this area. Low backscatter was also observed in the vicinity of this mooring during the survey (Fig. 2). The central mooring exhibited two periods of elevated backscatter, one in mid-late February prior to the increase in backscatter at the north mooring and again in late March after backscatter at the north mooring had peaked (Fig. 5B). Backscatter at the south mooring increased in late April after subsiding at the north and central moorings (Fig. 5). Backscatter at the south mooring remained relatively high until the end of April (Fig. 5 C). These patterns are consistent with those from the repeat coarse-scale surveys (Fig. 3) in that they suggest that pollock were moving from the central to the north part of the Strait in late February and early March, aggregating at high density in the vicinity of the north mooring in early March and then moving back past the central mooring in late March and south mooring in April. By early May, backscatter in Shelikof Strait was low (Figs. 2, 5).

2.3 Comparison of backscatter observed from ships and moorings

The observations from the echosounder moorings and survey vessels were similar, indicating that the moorings provided information that reflected pollock abundance over a much larger area than the relatively small area directly observed by the moored echosounder. The vessel observations from the 50 nmi^2 (171.7 km^2) small-scale surveys were highly correlated (natural-log transformed data, $r = 0.95$ $p < 0.001$) with the concurrent observations from the stationary moorings (Fig. 6). The ratio comparing the

38 kHz vessel observations to the concurrent 70 kHz moored echosounder observations indicated that the vessel/mooring ratio (i.e. $s_{A,vessel}$ /$s_{A,mooring}$) was 1.32 (95% CI 1.05-1.66). When adjusted for the mean vessel/mooring ratio, the vessel observations in the 50 nmi^2 survey area overlap with the hourly mooring observations (i.e. compare black symbols with grey lines in Fig. 5). Averaging the mooring observations over the period of the coarse-scale surveys produced a similar time series to that of the coarse scale-surveys (Fig. 7).

2.4 Retrospective analysis surveys to inform mooring placement.

The retrospective analysis indicated that a relatively small number of 'virtual moorings' can be used to generate an abundance index that tracks pollock backscatter in the Strait. As the number of moorings was increased from 1 to 5, the prediction errors generally declined (Fig. 8). The out-of-sample prediction error of survey backscatter from 1-2 moorings was relatively high (mean prediction errors of 44 and 58%, respectively, Figure 8). Although predictions from a single mooring were significantly correlated with the survey observations ($r = 0.78$, $p < 0.001$), those from 2 moorings, which are more variable, were not ($p > 0.05$).

In the case of 3 virtual moorings (Fig. 9A), the predictions were correlated with the survey observations ($r = 0.87$, $p < 0.001$). The 3-mooring prediction was improved relative to 1-2 moorings (mean error of 26%), but the errors remained high in some years (e.g. 1998 and 2005, Fig. 8). The optimal mooring locations ($n = 19$, one for each prediction) were clustered in 2-3 locations and the same location was selected 47-58% of the time, depending on the stratum (Fig. 9B). Thus, only a few combinations of sites were repeatedly identified as optimal mooring locations in the 19 model runs.

The locations of the 3 moorings deployed in 2015 were decided prior to the final retrospective analysis as the sampling area of the mooring had not been characterized. However, the retrospective analysis suggests that moorings in the deployment locations are likely to track abundance in the strait. Three virtual moorings in the deployment locations produced mean out-of-sample prediction errors of 29%, which is similar to the 26% observed for the 3 optimal locations selected in the analysis (Figure 8).

Four virtual moorings were also correlated with the survey observations (Fig. 9C, $r = 0.85$, $p < 0.001$), and resulted in similar prediction errors as 3 moorings, with slightly lower variability (Fig. 8). Again, a small subset of potential sites in each stratum were favored: a single site was selected 58-68% of the time, depending on the stratum (Fig. 9D). These locations were often the same as those selected in the 3-mooring model (i.e. compare Figs 9B and 9D).

In the 5-virtual mooring simulation, the prediction closely tracked the survey observations (Fig. 9E, $r = 0.98$, $p < 0.001$), and the mean prediction error fell to an average of 10.7% with a range of 0.9-22.8% (Fig. 8). In the 5-virtual mooring case, the same 5 locations were selected in all 19 model runs (Fig. 9F). The 5-virtual mooring sites produced relatively consistent model coefficients across out-of-sample runs (Table 1), indicating that the model results (coefficients and mooring sites) are not highly sensitive to the survey years used to predict suitable mooring locations. The mooring in stratum 4 has a high a coefficient indicating high influence (Table 1). This is likely because observations at this site tend to track the survey well over time (i.e. $s_{A.site}/s_{A,survey}$ has a low standard deviation, Table 1).

2.5 Prediction of survey backscatter from daily mooring observations

The three echosounder moorings deployed in Shelikof Strait were used along with the method described in section 1.6 to make daily predictions of backscatter in the Shelikof survey area. The predictions exhibit substantial temporal variability (Fig. 10, squares), particularly in mid to late March, when abundance at the mooring sites was changing rapidly (Fig. 5). However, when the daily observations are temporally averaged with a 15-day running mean, the observations in mid to late March are close to those observed in the survey, which occurred at this time (i.e. compare solid and dashed line in Fig. 10). When the mooring-based estimates are averaged over the 2015 survey duration (17-24 March) the average mooring-based prediction is 13.8% higher than the survey, and when averaged over the duration of historical surveys (13 March - 1 April), the prediction is 19.6% higher. Thus, although the moorings were not placed in optimal locations (i.e. compare Figs 1 and 9B), they produced reasonable estimates of survey backscatter when averaged over time. Additionally, the time-averaged mooring-based predictions are largely consistent with the temporal trends observed in the coarse-scale surveys (i.e. compare gray line and black circles in Fig. 10), which suggests that the mooring-based index is capturing the temporal trends in pollock abundance over a broad area.

Discussion

Measurements of pollock backscatter from bottom-moored echosounders were remarkably similar to those made by vessels surveying a much larger area. A mooring observes an area equivalent to that covered by a survey vessel in less than a minute, but does so repeatedly. For example, during the annual Shelikof Strait acoustic-trawl survey, the vessel's echosounder samples a volume ~16,000 times greater than a single mooring. Despite their smaller sampling area, the mooring observations were correlated with the concurrent 50 nmi^2 ship surveys, and observations from three moorings were consistent with ship-based surveys of the entire Strait. Thus, the upward-looking echosounders produced acoustic measures representative of fish abundance in areas that are much larger than those sampled in the beam.

In Shelikof Strait, a single mooring provided information on pollock backscatter comparable to that from a 50 nmi^2 vessel survey. We thus used survey information in a grid cell of this size to represent the information content of virtual moorings to simulate the performance of echosounder moorings in this environment. Analysis of a 19-year time series using survey data to represent 'virtual' moorings indicated that a relatively small number of moorings (3 or 5, ideally 5) will provide a useful acoustic index of the abundance of pre-spawning pollock. Increasing the numbers of virtual moorings did not always appreciably increase out-of-sample predictions of survey backscatter (e.g. 1 vs. 2 and 3 vs. 4 moorings), as the datasets used to fit the model are not the same as the withheld survey used to evaluate the success of the model (i.e. overfitting is occurring during model fitting). Thus, in the case of Shelikof Strait, there is only a marginal benefit to using 3 vs. 4 moorings, but there is a substantial improvement when 5 moorings are used. A simulated five mooring array reproduced the survey time series well, with mean prediction errors of <11%. It may thus be possible in certain situations (e.g. pre-spawning pollock in Shelikof Strait) to derive indices of abundance over wide areas with a small number of moorings.

The observations from the three moorings deployed in 2015 also support the inference that a small number of moorings can be used to produce an index of pollock abundance in Shelikof Strait. The three moorings exhibited substantial short-term variability, largely due to the rapid changes in abundance as the fish moved through the strait, but produced abundance estimates that were within those expected from the retrospective analysis when averaged over the duration of the annual survey. As discussed below, these observations would likely have been less variable if the moorings had been deployed in model-selected locations.

The mooring-derived estimate depends on the empirically-derived conversion between mooring and ship measurements, which have different transducer orientations and operating frequencies. Inaccuracies in this conversion will cause mooring-based estimates to differ consistently from ship estimates. This bias will be less of a concern in applications where the mooring-based time series is treated as an index proportional to population size. For applications sensitive to this conversion (e.g. combining data from ships and moorings), these uncertainties can be reduced by additional ship-mooring comparisons, or determination of fish target strength as a function of frequency and orientation.

The retrospective analysis provided an objective framework to evaluate the effectiveness of potential configurations of a moored echosounder array for prediction of acoustic backscatter from pre-spawning pollock. The analysis provided insight as to the number of moorings needed, where they should be deployed, and how the data from multiple echosounders can be combined into an abundance index. The approach is similar to survey optimizations in which historical spatial distributions are used to evaluate the accuracy and precision of various sampling designs (e.g. Liu et al., 2009). The methods employed here are also similar to observing system simulation experiments (OSSEs), an approach used to plan meteorological observing networks (Arnold and Dey, 1986). OSSE's have been used to design oceanographic mooring arrays by evaluating the ability of multiple moorings to reproduce spatial observations (Hackert et al., 1998; Ballabrera-Poy et al., 2007).

It is striking that in Shelikof Strait, a small subset of possible mooring locations was highly favored over others. In the case of 5 moorings, the same locations were selected in all 19 out-of-sample runs. These locations (or adjacent ones) were often selected when fewer virtual moorings were considered, which further indicates that these sites are favorable mooring locations. The exhaustive search used to evaluate mooring locations was effective for the purposes of this study, but it does not scale well as the number of combinations to be tested increases steeply with the number of moorings considered. More efficient optimization methods (e.g. selecting additional moorings in a sequential fashion, Ballabrera-Poy et al., 2007) or simplifying assumptions (e.g. testing fewer or a coarser grid of potential locations) would likely be required if more moorings are considered.

Mooring locations were identified based on historical information, and an abundance index derived from these locations will be sensitive to changes in the distribution of pollock. If the distribution of the population shifts dramatically to one that was not well-represented in the historical training data set, the optimal mooring locations may not capture the abundance well in that year. This constraint is not unique to echosounder moorings. Ship-based surveys are subject to similar biases as populations can move in and out of the survey area. Models trained on data will be less reliable if the training data are not representative of the conditions under which predictions are made (Vaughan and Ormerod, 2003). This can be exacerbated if certain locations are heavily weighted (e.g. high *a* in eq. 2). However, one can likely identify an anomalous population distribution by monitoring the proportion of backscatter observed at the different mooring sites. A shift in the proportion of backscatter observed among mooring sites can be used as an indication that a mooring-based abundance index should be interpreted with caution. For example, in 2016, the survey indicated that pollock were anomalously distributed at the time of the survey (Fig. S3A), and as expected, predictions were not as good as in most other years (Fig. S3B). However, the virtual mooring abundance index was still within the upper end of the range observed in previous model runs (Fig. S3B), suggesting that the predictions are robust to changes in distribution of this magnitude.

Our initial intuition was to place moorings in the areas of highest historical abundance. However, the retrospective analysis indicates that areas with lower variance may be more favorable sites for echosounder moorings. For example, in the 5-mooring model, site 4 is weighted heavily. Although abundance at this location is relatively low, a consistent proportion of the backscatter is observed at this location. The retrospective analysis may select against high-abundance spawning areas even if fish aggregate annually at these sites if the aggregations are not observed on all surveys. For example, the north mooring was deployed in a suspected spawning area where high densities of pre-spawning adult pollock are often detected on the annual survey (Wilson, 1994), but this site is not optimal as the time series is highly variable. The mooring record (Figs. 4, 5A) indicates that although backscatter at the north mooring site was low at the time of the 2015 survey, it had been ~15 times higher a week prior to the survey. The survey was not well-timed with respect to the formation of the spawning aggregation in this specific location (however, the fish were likely in the adjacent areas covered by the survey). Areas exhibiting rapid changes in density will increase the variability of mooring-based abundance indices, and they are thus less likely to be identified as favorable mooring locations in our analysis.

In addition to producing abundance estimates, the 3 moorings documented the formation and dispersal of pollock spawning aggregations in Shelikof Strait. The abundance index generated from the 3 moorings differs from the time series observed in individual moorings, which reflect local events as the fish migrate through the Strait. Survey timing has been demonstrated to be the major source of uncertainty in some surveys of spawning fish (e.g., O'Driscoll, 2004), and optimizing survey timing is difficult because the timing of spawning aggregations can be variable (e.g., Lawson and Rose, 2000). Repeated surveys of Shelikof Strait have revealed that pollock abundance can change substantially over ~2 week periods during the spawning period (Nelson and Nunnallee, 1984, Wilson, 1994). Moored echosounders can be averaged over long periods of time (a spawning season), which reduces the impacts of short-term variability (e.g. behaviors altering target strength or detectability) and temporal mismatches on abundance indices.

The abundance indices derived from the moorings and the coarse-scale surveys indicate that the March timing of the Shelikof Strait acoustic-trawl survey is reasonable. This work supports a previous study which concluded based on repeated surveys and analyses of fish maturity state that a mid-to-late March survey in Shelikof Strait is appropriate (Wilson, 1994). The moorings indicate that pollock abundance begins to decrease in early April, and a survey after late March would be questionable. Direct measurement of the timing of spawning aggregations represents an improvement to monitoring the proportion of fish in spawning condition as an index of survey timing, as reproductive state is not necessarily related to abundance at spawning sites (Lawson and Rose, 2000). Although appropriate survey timing can be estimated with repeat surveys (Wilson, 1994; O'Driscoll, 2004), there have been no repeat surveys of pre-spawning pollock in Alaska since 1994 due to the expense. In many cases, the timing of fish aggregations subject to acoustic surveys is a source of uncertainty, and observations with echosounder moorings can be used to establish the appropriate time to conduct these surveys.

A principal limitation of autonomous acoustic applications such as bottom-moored echosounders is that they measure acoustic backscatter, which although useful in some applications (Benoit-Bird and Au, 2002; Honkalehto et al., 2011; Melvin et al., 2016) is not equivalent to the typical output (abundance by species/age/size class) of traditional surveys (Simmonds and MacLennan, 2005). Identification of the primary sound scatters is not a major concern in Shelikof Strait, as in early spring, backscatter is dominated by spawning pollock. However, this may be a key limitation in other situations. An important area for further development of fisheries acoustics on moorings and other autonomous platforms (Guihen et al., 2014; Meyer-Gutbrod et al., 2015) is the development of methods to incorporate ancillary information about species composition and size structure (e.g. fishery catches, stock assessment model predictions), and to exploit other sources of information contained in the acoustic signal [e.g. target strength, (Traynor, 1996), schooling characteristics (Kaltenberg et al., 2010), frequency response (Korneliussen and Ona, 2003; Ross et al., 2013; Stanton et al., 2012)]. However, these ancillary measures will likely be most effective when supplemented with independent sources of information such as trawl or optical sampling. This can be accomplished via periodic sampling, and it may be possible to incorporate optical instruments that can be used to identify sound scatters and provide size information into the moorings (O'Driscoll et al., 2012; Williams et al., 2014). The degree to which the backscatter measurements can be interpreted in biologically meaningful ways is a key issue when considering the use of moored echosounders.

The extent to which observations from moorings can be extrapolated over wider spatial areas will depend on the species present, their behavior, and the environment. In situations where animals are relatively stationary, repeated samples from a moored instrument over time will contain little additional information as the observations represent the abundance over a very small area, particularly if the distributions are patchy as for schooling fishes. However, when organisms move relative to the moored echosounder beam due to the combined effects of swimming and advection, the measurements from the moorings will represent abundance over a broader spatial scale

(Brierley et al., 2006). Shelikof Strait is a favorable environment for observation of fish from echosounder moorings as the backscatter during the spawning season is dominated by walleye pollock, which aggregate in widespread and homogenous layers (McCarthy et al., 2015). In the spring, the population migrates through the strait and there is significant potential for advection in the south-west flowing Alaska Coastal Current (Reed and Bograd, 1995), which may increase the transport of fish past the stationary echosounders.

This work indicates that despite the modest volumes sampled by stationary echosounders, it is possible to derive quantitative indices of abundance from a relatively sparse array of echosounder moorings deployed over a wide area. However, it is important to recognize that this technique does not produce an index of abundance-at-size or age and other biological information (weight-length relationships, maturity state) produced by a traditional survey, and the consequences of this must be considered for a given application. This work was focused on the potential to derive quantitative abundance indices from a small number of bottom-moored echosounders in a specific survey area, but the approach is generally applicable. The degree to which stationary echosounders represent the abundance of organisms outside of the directly observed volume is broadly relevant to the use of these instruments. Stationary echosounders are often used in behavioral studies, and the observations from these instruments are (often implicitly) attributed to the population as a whole. The technology for quantitative acoustic measurements from the seafloor is relatively well-developed, and the primary challenge is how to apply these methods most effectively. Survey time series can be used to objectively estimate the number and placement of moorings required to derive a useful index of abundance, and to formulate a method to combine observations from multiple moorings into an abundance index. In this fashion, the potential benefit of this approach can be explored in a cost-effective manner, and the utility of long-term observations from stationary echosounders can be maximized.

Acknowledgements

Ivar Wangen and Lars Andersen designed the WBAT and moved mountains to ensure a successful deployment. The captain and crew of the F/V *Mar Del Norte* and the NOAA Ship *Oscar Dys*on and members of the fisheries acoustics program at the Alaska Fisheries Science Center made the field work possible. The work was funded by NOAA's Office of Science and Technology and Cooperative Research Programs. Reference to trade names does not imply endorsement by NOAA.

References

Arnold, C. P., and Dey, C. H. 1986. Observing-systems simulation experiments - past, present, and future. Bull. Am. Meteorol. Soc., 67: 687-695.

Ballabrera-Poy, J., Hackert, E., Murtugudde, R., and Busalacchi, A. J. 2007. An observing system simulation experiment for an optimal moored instrument array in the tropical Indian Ocean. J. Climate, 20: 3284-3299.

Benoit, D., Simard, Y., and Fortier, L. 2008. Hydroacoustic detection of large winter aggregations of Arctic cod (*Boreogadus saida*) at depth in ice-covered Franklin Bay (Beaufort Sea). J. of Geophys. Res. Oc. Atm., 113: 2156-2202.

Benoit-Bird, K. J., and Au, W. W. 2002. Energy: Converting from acoustic to biological resource units. J. Acoust. Soc. Am. 11: 2070-2075.

Brierley, A. S., Saunders, R. A., Bone, D. G., Murphy, E. J., Enderlein, P., Conti, S. G., and Demer, D. A. 2006. Use of moored acoustic instruments to measure short-term variability in abundance of Antarctic krill. Limnol. Oceanog. Methods, 4: 18-29.

Demer, D.A., Berger, L., Bernasconi, M., Bethke, E., Boswell, K., Chu, D., Domokos, R., *et al*. 2015. Calibration of acoustic instruments. ICES Cooperative Research Report No. 326: 133 pp.

De Robertis, A., Taylor, K., Wilson, C., and Farley, E. 2017. Abundance and distribution of Arctic cod (*Boreogadus saida*) and other pelagic fishes over the U.S. Continental Shelf of the Northern Bering and Chukchi Seas Deep Sea Res. Part II Top. Stud. Oceanogr. 135: 51-65.

Doonan, I. J., Bull, B., and Coombs, R. F. 2003. Star acoustic surveys of localized fish aggregations. ICES J. Mar. Sci., 60: 132-146.

Dorn, M., Adyin, K., Jones, D., McCarthy, A., Palsson, W., and Spadlinger, K. 2015. Assessment of the Walleye Pollock Stock in the Gulf of Alaska. 172 pp. North Pacific Groundfish Stock Assessment and Fishery Evaluation Report. http://www.afsc.noaa.gov/REFM/Docs/2015/GOApollock.pdf.

Guihen, D., Fielding, S., Murphy, E. J., Heywood, K. J., and Griffiths, G. 2014. An assessment of the use of ocean gliders to undertake acoustic measurements of zooplankton: the distribution and density of Antarctic krill (E*uphausia superba*) in the Weddell Sea. Limnol. Oceanog. Methods, 12: 373-389.

Hackert, E. C., Miller, R. N., and Busalacchi, A. J. 1998. An optimized design for a moored instrument array in the tropical Atlantic Ocean. J. Geophys. Res, 103: 7491-7509.

Honkalehto, T., Ressler, P. H., Towler, R., and Wilson, C. D. 2011. Using acoustic data from fishing vessels to estimate walleye pollock abundance in the eastern Bering Sea. Can. J. Fish. Aquat. Sci., 68: 1231-1242.

Kaartvedt, S., Rostad, A., Klevjer, T. A., and Staby, A. 2009. Use of bottom-mounted echo sounders in exploring behavior of mesopelagic fishes. Mar. Ecol. Prog. Ser., 395: 109-118.

Kaltenberg, A. M., Emmett, R. L., and Benoit-Bird, K. J. 2010. Timing of forage fish seasonal appearance in the Columbia River plume and link to ocean conditions. Mar. Ecol. Prog. Ser., 419: 171-184.

Kieser, R., Mulligan, T. J., Williamson, N. J., and Nelson, M. O. 1987. Intercalibration of two echo integration systems based on acoustic backscattering measurements. Can. J. Fish. Aquat. Sci., 44: 562-572.

Korneliussen, R. J., and Ona, E. 2003. Synthetic echograms generated from the relative frequency response. ICES J. Mar. Sci., 60: 636-640.

Lawson, G. L., and Rose, G. A. 2000. Small-scale spatial and temporal patterns in spawning of Atlantic cod (*Gadus morhua*) in coastal Newfoundland waters. Can J. Fish. Aquat. Sci., 57: 1011-1024.

Løland, A., Aldrin, M., Ona, E., Hjellvik, V., and Holst, J. C. 2007. Estimating and decomposing total uncertainty for survey-based abundance estimates of Norwegian spring-spawning herring. ICES J. Mar. Sci., 64: 1302-1312.

MacLennan, D. N., Fernandes, P. G., and Dalen, J. 2002. A consistent approach to definitions and symbols in fisheries acoustics. ICES J. Mar. Sci., 59: 365-369.

Liu, Y., Chen, Y., and Cheng, J. 2009. A comparative study of optimization methods and conventional methods for sampling design in fishery-independent surveys. ICES J. Mar. Sci., 66: 1873-1882.

McCarthy, A. L., Stienessen, S. C., and Jones, C. 2015. Results of the acoustic trawl surveys of walleye pollock (*Gadus chalcogrammus*) in the Gulf of Alaska, February-March 2014 (DY2014-01 and DY2014-03). AFSC Processed Rep. 2015-05, 85 p. https://www.afsc.noaa.gov/Publications/ProcRpt/PR2016-01.pdf

Melvin, G. D., Kloser, R., and Honkalehto, T. 2016. The adaptation of acoustic data from commercial fishing vessels in resource assessment and ecosystem monitoring. Fish. Res., 178: 13-25.

Meyer-Gutbrod, E. L., Greene, C. H., and McGarry, L. P. 2015. Wave Glider Technology for Fisheries Research. Sea Technology, December 2015, 15-19.

Nelder, J. A., and Wedderburn, R. W. M. 1972. Generalized Linear Models. Journal of the Royal Statistical Society Series A (General), 135: 370-384.

Nelson, M. O., and Nunnallee, E. P. 1984. Results of the acoustic-midwater trawl surveys of spawning pollock in the Shelikof Strait region of the Gulf of Alaska during 1980-81 and 1983-84. NOAA Technical Memorandum F/NWC-80. 30 pp.

O'Driscoll, R. L. 2004. Estimating uncertainty associated with acoustic surveys of spawning hoki (*Macruronus novaezelandiae*) in Cook Strait, New Zealand. ICES J. Mar. Sci., 61: 84-97.

O'Driscoll, R. L., de Joux, P., Nelson, R., Macaulay, G. J., Dunford, A. J., Marriott, P. M., Stewart, C., et al. 2012. Species identification in seamount fish aggregations using moored underwater video. ICES J. Mar. Sci, 69: 648-659.

Reed, R. K., and Bograd, S. J. 1995. Transport in Shelikof Strait, Alaska - an Update. Cont. Shelf Res., 15: 213-218.

Ross, T., Keister, J. E., and Lara-Lopez, A. 2013. On the use of high-frequency broadband sonar to classify biological scattering layers from a cabled observatory in Saanich Inlet, British Columbia. Methods in Oceanography, 5: 19-38.

Simmonds, E. J., and MacLennan, D. N. 2005. Fisheries Acoustics 2nd. Ed. Blackwell Science LTD, Oxford, UK. 437 p.

Stanton, T. K., Sellers, C. J., and Jech, J. M. 2012. Resonance classification of mixed assemblages of fish with swimbladders using a modified commercial broadband acoustic echosounder at 1-6 kHz. Can. J. Fish. Aquat. Sci., 69: 854-868.

Traynor, J. J. 1996. Target strength measurements of walleye pollock (*Theragra chalcogramma*) and Pacific whiting (*Merluccius productus*). ICES J. Mar. Sci., 53: 253-258.

Trevorrow, M. V. 2005. The use of moored inverted echo sounders for monitoring meso-zooplankton and fish near the ocean surface. Can. J. Fish. Aquat. Sci., 62: 1004-1018.

Vaughan, I. P., and Ormerod, S. J. 2003. Improving the quality of distribution models for conservation by addressing shortcomings in the field collection of training data. Conserv. Biol., 17: 1601-1611.

Wessel, P., and W. H. F. Smith, A, 1996. Global Self-consistent, Hierarchical, High-resolution Shoreline Database, J. Geophys. Res., 101, #B4, pp. 8741-8743.

Williams, K., De Robertis, A., Berkowitz, Z., Rooper, C., and Towler, R. 2014. An underwater stereo-camera triggered by the presence of animals. Methods in Oceanography, 11: 1-12.

Wilson, C. D. 1994. Echo integration-trawl survey of pollock in Shelikof Strait, Alaska in 1994. Appendix D in Stock Assessment and Fishery Evaluation report for the groundfish resources of the Gulf of Alaska for 1995. North Pacific Fishery Management Council. Anchorage AK. p. 1-39.

Canadian Journal of Fisheries and Aquatic Sciences

Table 1. Locations and depths of mooring sites selected in the 5-mooring retrospective analysis (i.e. Fig. 9F in text). The mean ratio between the average nautical area backscattering coefficient observed at these sites, and the survey wide-average ($s_{A,site}$ / $s_{A,survey}$) and the standard deviation computed across years is given. The mean model coefficient (*a*, see eq. 2) and the range of model coefficients observed in the 19 out-of-sample runs are listed.

Mooring Number	Latitude (°N)	Longitude (°W)	Depth (m)	$s_{A,site}$ / $s_{A,survey}$ mean (SD)	Model coefficient mean (low/high)
1	57.8117	-154.1667	233	0.87 (0.83)	0.1254 (0.1060/0.1374)
2	57.8123	-154.9265	305	2.50 (1.74)	0.0387 (0.0295/0.0429)
3	57.6419	-155.3150	337	2.79 (2.04)	0.0453 (0.0404/0.0514)
4	56.9775	-155.3990	266	1.12 (0.52)	0.4122 (0.3997/0.4282)
5	56.2696	-156.2651	268	1.17 (1.05)	0.1641 (0.1547/0.1893)

Figure Legends

Fig. 1. Study area in Shelikof Strait. The locations of the echosounder moorings are indicated by gray dots. Survey transects are shown as black lines and the 5 transects comprising the coarse-scale survey are indicated by thick gray lines. The inset shows the ship track during a small-scale mooring survey, with the mooring location indicated by the grey circle. A trawl haul was conducted each time a mooring was visited. The 200 m depth contour is indicated by the light gray lines. Map data on this and subsequent maps are from Wessel and Smith (1996).

Fig. 2. Acoustic backscatter (s_A, m^2 nmi^{-2}) observed during the 2015 acoustic-trawl survey in Shelikof Strait. The height of each bar corresponds to the observed pollock backscatter. Transects comprising the coarse-scale survey are depicted in black, others in grey. The locations of the echosounder moorings are indicated by gray circles, and the 200 m depth contour is indicated by light gray lines. A scale bar is provided at the bottom of the figure.

Fig. 3. Acoustic backscatter observed during the coarse-scale surveys of Shelikof Strait. The 200 m depth contour is indicated by light gray lines. The height of each bar corresponds to the observed backscatter. The survey date and mean nautical area backscattering coefficient (s_A, m^2 nmi^{-2}), are listed on each panel.

Fig. 4. Echograms from the north mooring highlighting the rapid changes in pollock abundance and distribution at this site. The records start at 12:00 UTC on the dates indicated and last 400 s.

Fig. 5. Time series of backscatter at the A) north B) central and C) south mooring sites. The light gray lines indicate the average of the 200 ping ensembles collected hourly, the darker gray lines and circles give the daily averages. The black symbols indicate the average backscatter observed during the ship-based survey in the vicinity of the mooring. The ship measurements have been scaled to account for differences in frequency (38 vs. 70 kHz) and observation geometry (i.e. down vs. up-looking). This was done by multiplying the 38 kHz ship backscatter by 0.76, which corresponds to the reciprocal of the mooring/ship ratio described in section 2.3. The error bars, which in some cases are not visible, represent the 95% confidence intervals estimated for this ratio. Note the different scales for each panel and the scale breaks.

Fig. 6. Relationship between the backscatter observed by the echosounder moorings and survey vessels over the same time period presented on a natural-log scale. Each data point represents the average of observations over the duration of a 50 nmi^2 small-scale ship survey in the vicinity of a mooring (n=16). The open circles represent the observations in May when the moorings sampled once every 6 hours rather than once per hour. The dashed line represents the fitted vessel/mooring ratio of 1.32.

Fig. 7 Backscatter from moorings and the coarse-scale surveys. The coarse-scale survey is the mean backscatter observed during the 5-transect surveys depicted in Fig. 3. The 3-mooring average is the mean backscatter observed by the 3 echosounder moorings over the duration of the coarse-scale survey. The backscatter measurements of each type have been normalized to a mean of 1.

Fig. 8. Prediction error of out-of-sample predictions of observed survey backscatter decreases with the number of virtual moorings considered in the retrospective analysis. The prediction error is expressed as the absolute value of the percent difference from the survey observation in a given year (n=19). The box plots demarcate the 10^{th}, 25^{th}, 50^{th}, 75^{th} and 90^{th} percentiles of the prediction error, with the minimum and maximum depicted as black circles and the mean as an open circle.

Fig 9. Results of retrospective analysis using historical survey data as a proxy for observations from echosounder moorings. A-B) 3 virtual mooring sites, C-D) 4 virtual mooring sites, E-F) 5 virtual mooring sites. Panels to the left show the mean backscatter observed on the survey and the out-of-sample predictions (i.e. with the year being predicted excluded from the training set) for 'virtual moorings'. Panels to the right give the optimal locations established for the virtual moorings. Strata are color-coded, and the size of the symbol is proportional to the number of times a given location was selected as an optimal location in the 19 out-of-sample predictions.

Fig.10. Estimates of backscatter in Shelikof Strait derived from the 3 bottom-moored echosounders deployed in 2015. Daily backscatter estimates for the Shelikof Strait survey area (open squares) were generated by combining the average daily backscatter from individual moorings (eq. 4). These observations are averaged over time as a 15 day running mean (grey line), over the 2015 survey duration (17-24 March), and over the historical range of the Shelikof Strait survey dates (13 March to 1 April). Ship-based estimates of backscatter from the 2015 acoustic survey (dashed line) and survey-wide predictions from the four coarse-scale surveys during this period (black circles: details in Fig. S1) are given for comparison.

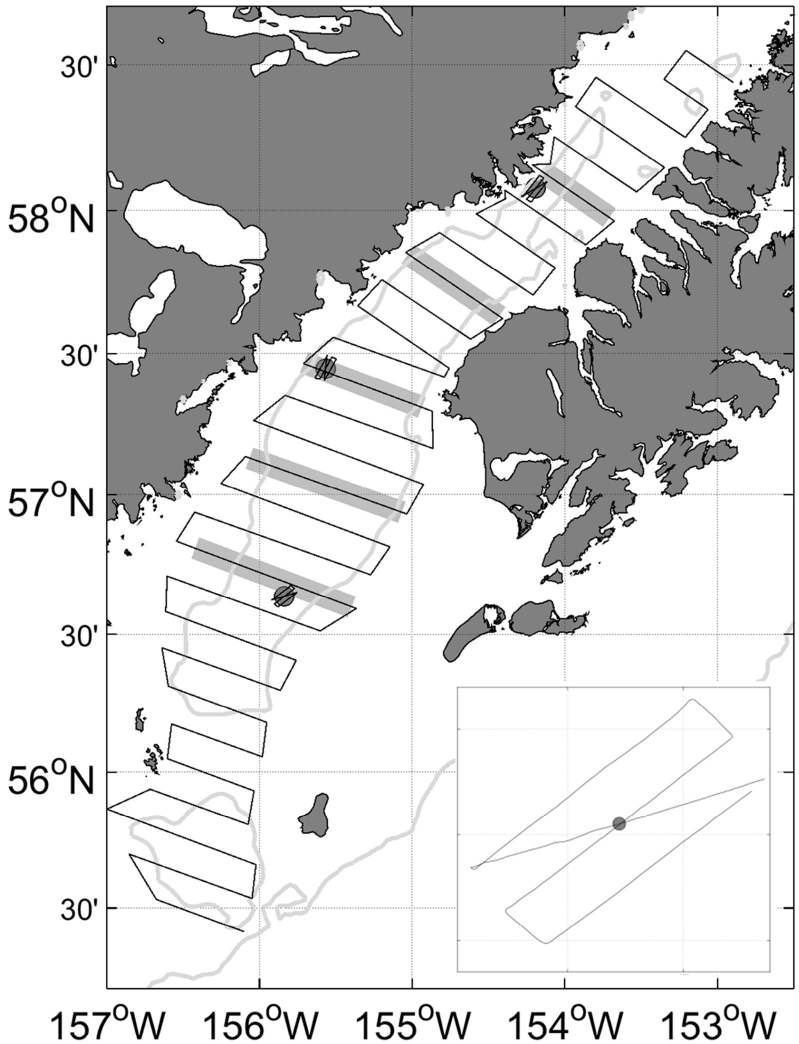

Fig. 1

123x151mm (279 x 279 DPI)

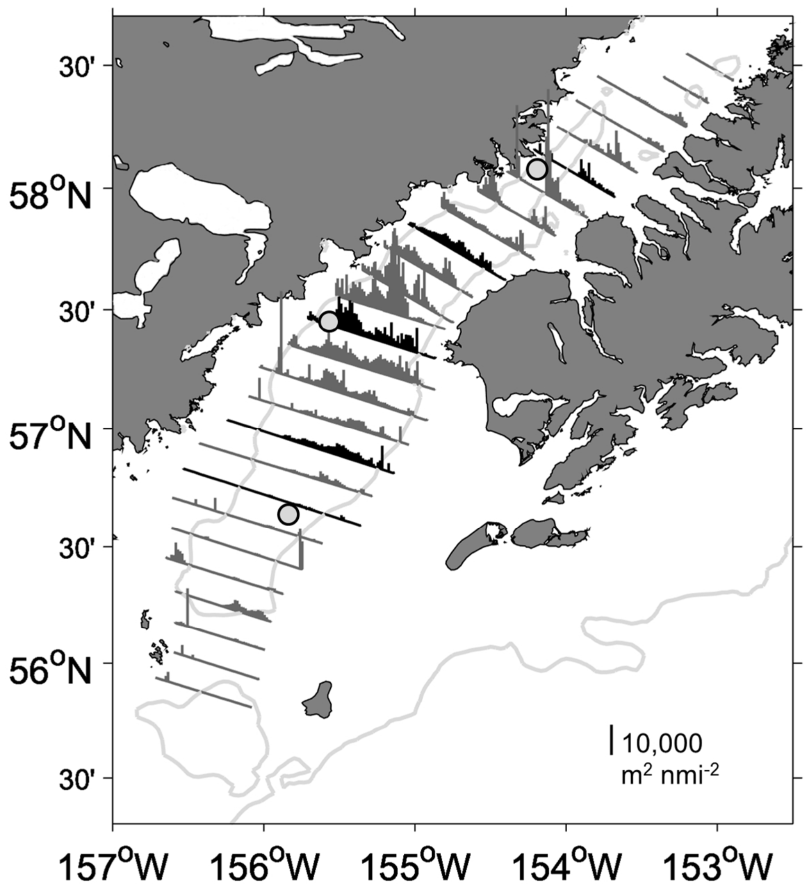

Fig. 2

133x146mm (279 x 279 DPI)

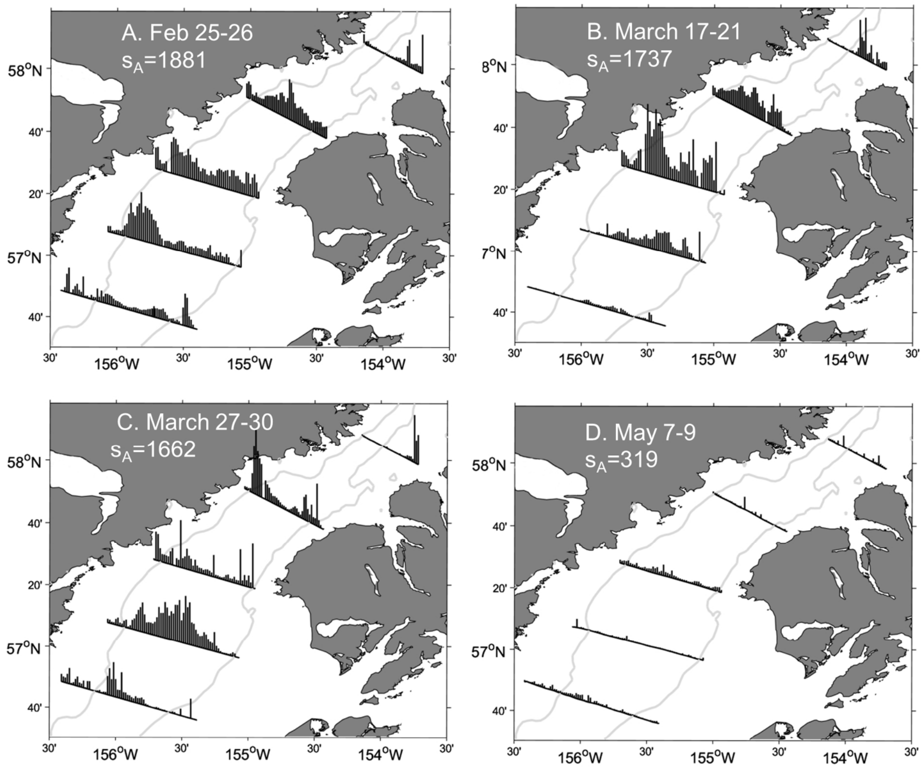

Fig. 3

186x163mm (279 x 279 DPI)

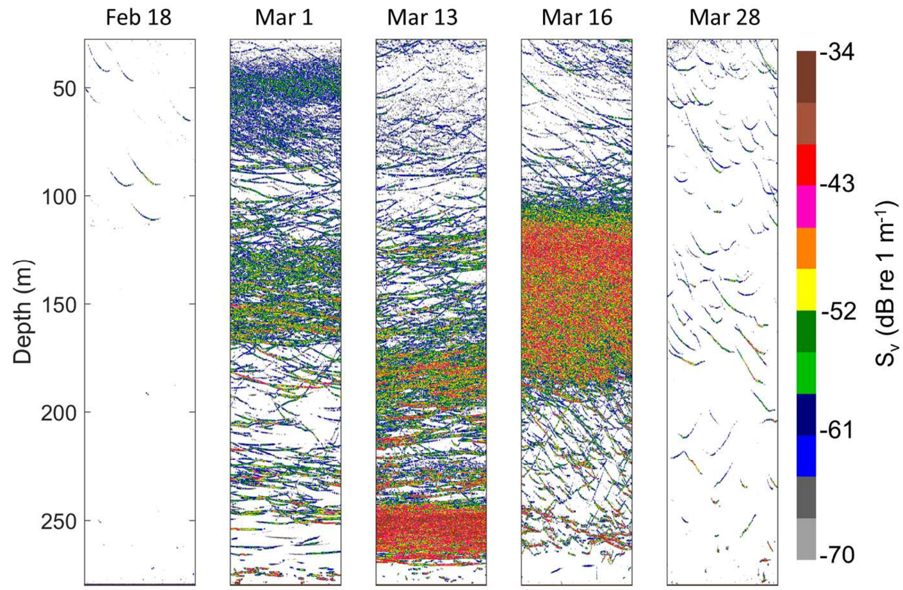

Fig. 4

173x120mm (279 x 279 DPI)

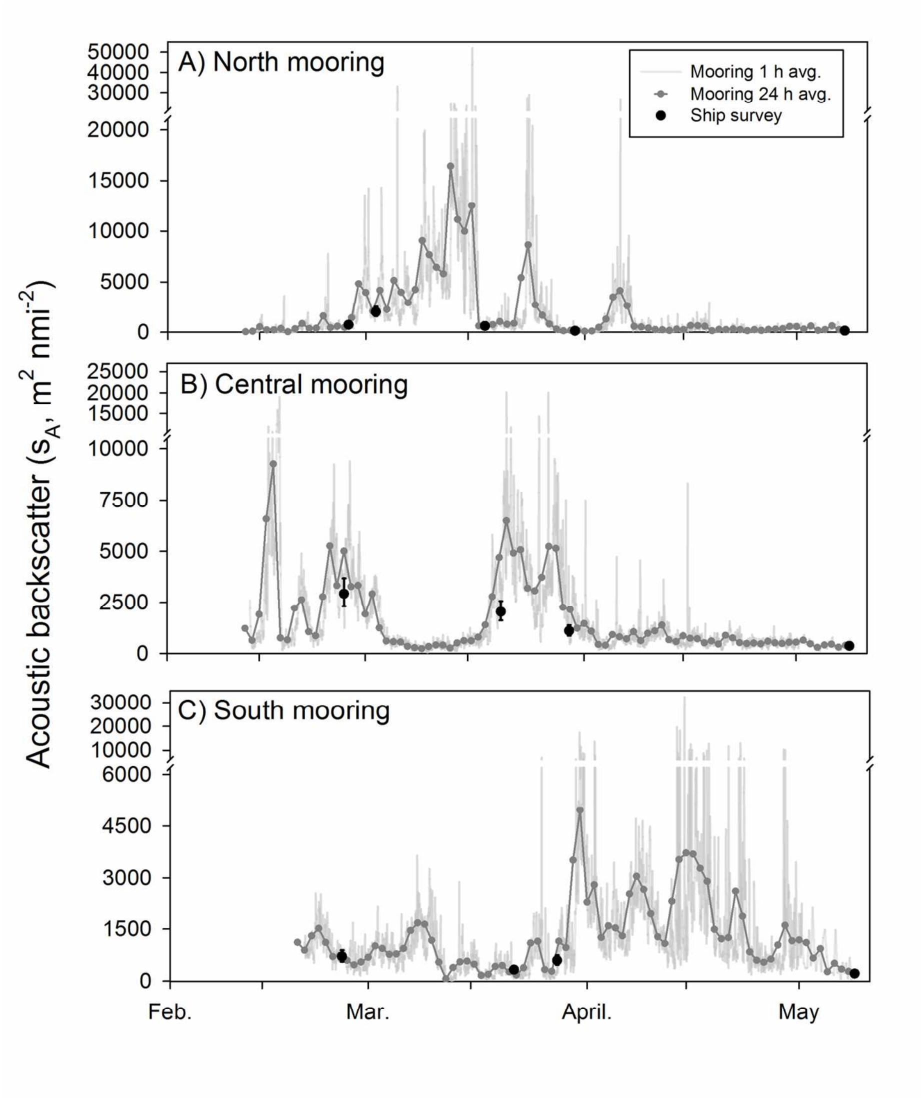

Fig. 5

166x183mm (279 x 279 DPI)

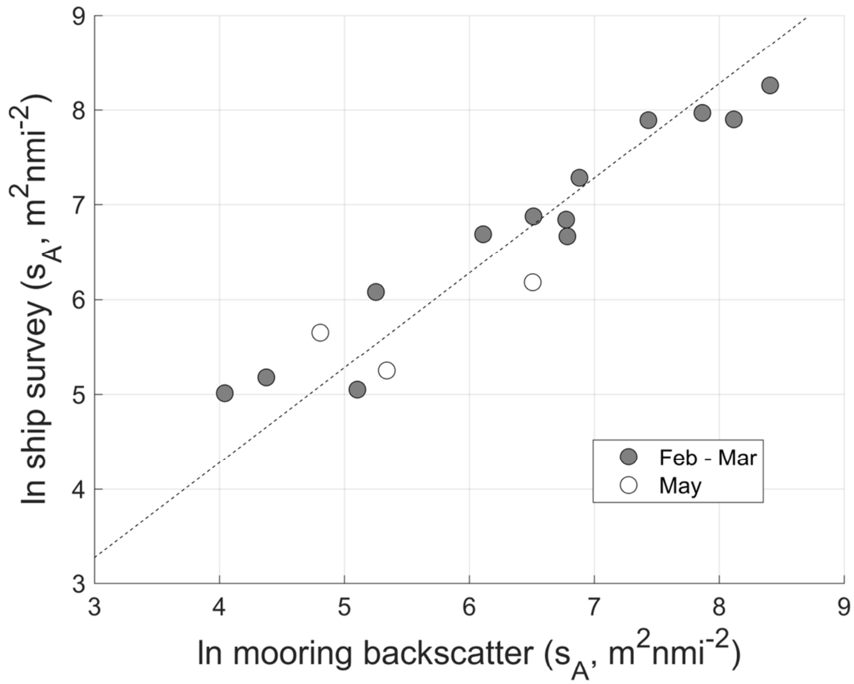

Fig. 6

172x141mm (279 x 279 DPI)

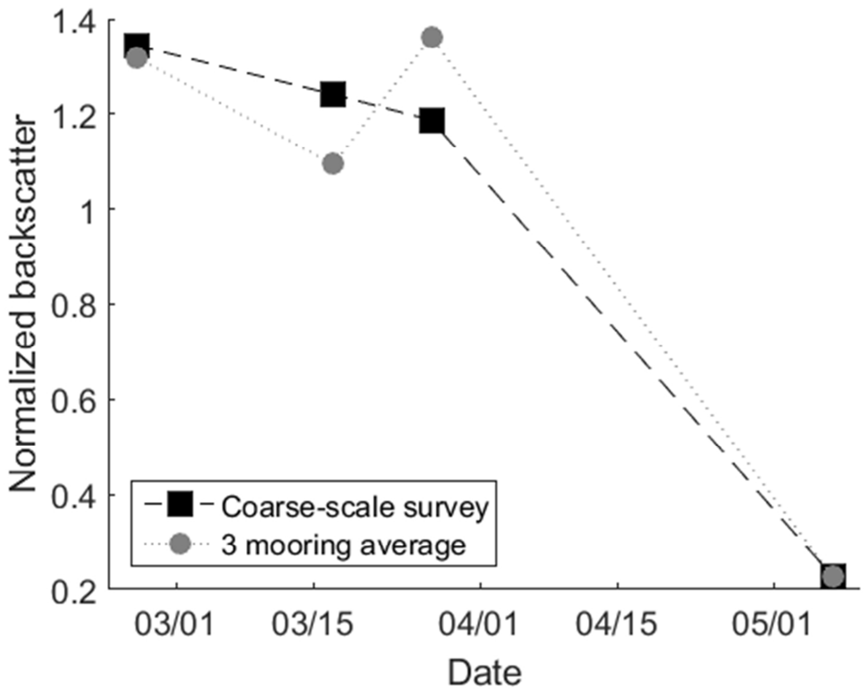

Fig. 7

152x121mm (279 x 279 DPI)

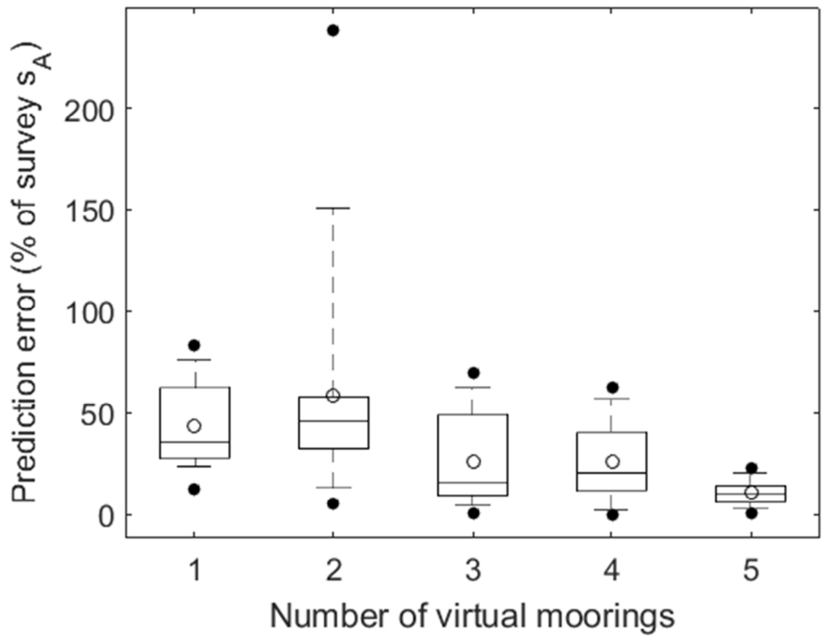

Fig. 8

163x125mm (279 x 279 DPI)

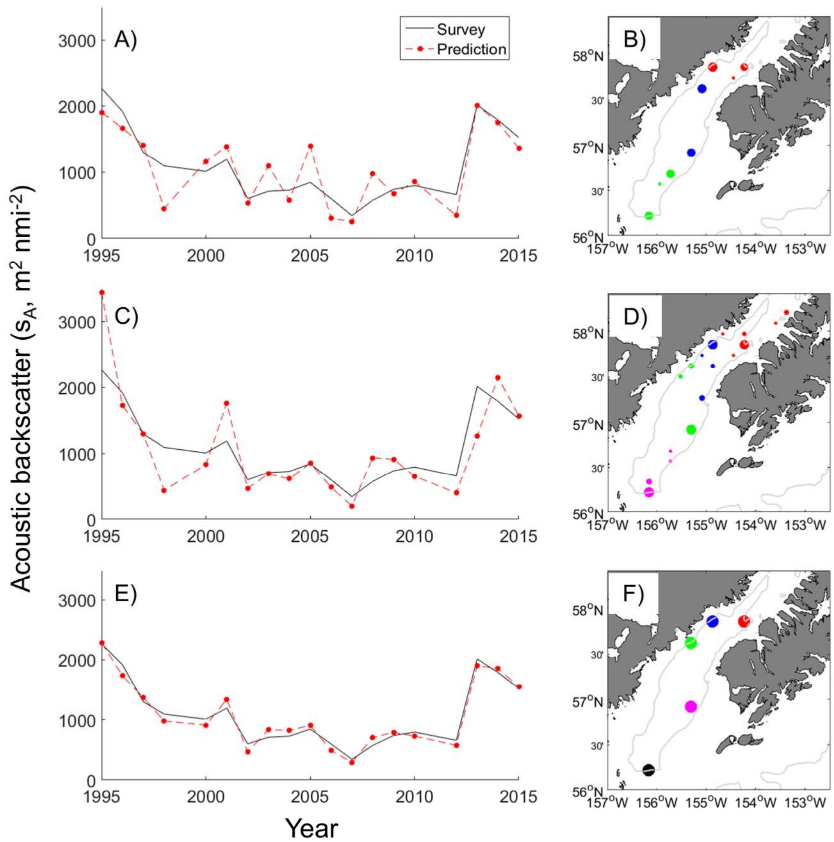

Fig. 9

184x175mm (279 x 279 DPI)

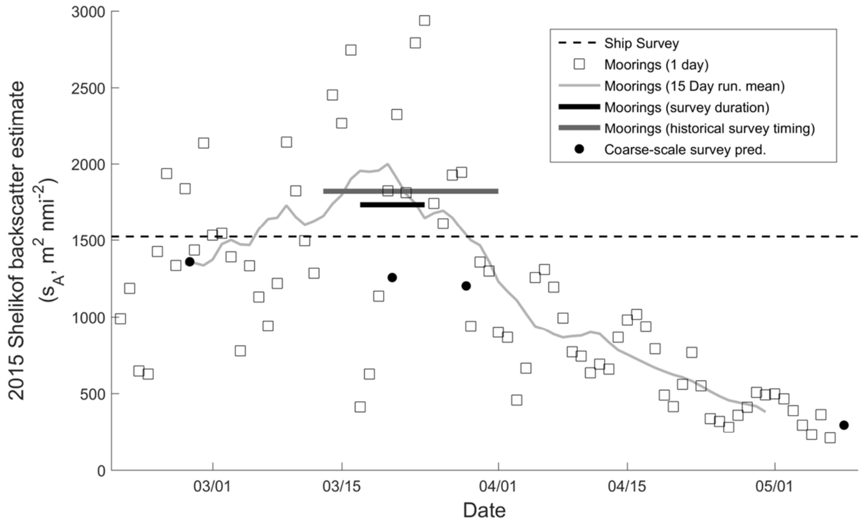

Fig. 10

186x114mm (279 x 279 DPI)